DALTON
FULL PAPER

Synthesis and characterisation of a Ru^{II}([14]aneS_4) complex immobilised in MCM-41-type mesoporous silica

Martyn Pillinger,[a] Isabel S. Gonçalves,*[a] André D. Lopes,[a] João Madureira,[a] Paula Ferreira,[a] Anabela A. Valente,[a] Teresa M. Santos,[a] João Rocha,*[a] Jorge F. S. Menezes[b] and Luís D. Carlos[b]

[a] *Department of Chemistry, University of Aveiro, 3810-193, Aveiro, Portugal. E-mail: igoncalves@dq.ua.pt*
[b] *Department of Physics, University of Aveiro, 3810-193, Aveiro, Portugal*

Received 5th February 2001, Accepted 4th April 2001
First published as an Advance Article on the web 24th April 2001

Ruthenium(II) complexes containing the macrocycle 1,4,8,11-tetrathiacyclotetradecane ([14]aneS_4) and nitrogen-coordinated nitrile ligands were prepared using *cis*-[Ru(DMSO)$_4$Cl$_2$] as the starting material. The first synthetic step consisted of introduction of the thioether ligand to give [Ru([14]aneS_4)(DMSO)Cl]Cl. Substitution of the DMSO ligand by the nitrile ligands $NCCH_3$ or $NC(CH_2)_3Si(OEt)_3$ (L) gave the complexes [Ru([14]aneS_4)(L)Cl]X (X = Cl^-, PF_6^-). Introduction of the triethoxysilyl ligand allowed the [Ru([14]aneS_4)Cl]$^+$ fragment to be tethered to the surface of the ordered mesoporous silica MCM-41 by pore volume impregnation of a solution of the complex in dichloromethane. A high metal loading was achieved (0.56 mmol g^{-1}). Powder XRD and N_2 adsorption studies of the derivatised material indicated that the textural properties of the support were preserved during the grafting experiment and that the channels remained accessible, despite a large reduction in both surface area and pore volume (*ca.* 50%). IR, UV/VIS, photoluminescence and MAS NMR spectroscopy (^{13}C, ^{29}Si) confirmed that the structural integrity of the Ru^{II} complex was retained during immobilisation, except for loss of ethoxide groups due to the reaction with pendant silanols on the silica surface.

Introduction

The confinement of transition-metal complexes within the constrained environment of periodic mesoporous oxides is an area of investigation that has blossomed since the discovery by researchers at the Mobil Corporation of the M41S family of micelle-templated silicas.[1] MCM-41, one member of this family, is particularly suitable as a support material owing to its high thermal stability, high surface area (1000 m^2 g^{-1}), high pore volume (1 cm^3 g^{-1}) and very narrow pore size distribution, tuneable in the range 20–100 Å.[2] A structural model for MCM-41 consists of a hexagonal arrangement of cylindrical pores embedded in a matrix of amorphous silica.

MCM-41-type mesoporous silicas may be derivatised using the same post-synthesis modification steps commonly used for amorphous oxide support materials. Thus, catalytically active sites and photo- and electro-active species can be incorporated within the mesopore by either primary or secondary (and higher order) grafting methods. Primary modifications entail one-step functionalisation by reaction of organometallic or metallo-organic compounds with the nucleophilic silanol groups present on the channel walls of MCM-41. Examples include reactions with $Mn_2(CO)_{10}$,[3] Cp_2TiCl_2,[4] [$SiMe_2(\eta^5$-$C_5H_4)_2$]$TiCl_2$,[5] [$Fe(\eta^5$-$C_5H_4)_2SiMe_2$],[6] and multiply-bonded dimolybdenum complexes.[7]

Ruthenium(II) polypyridyl complexes such as [Ru(bpy)$_3$]Cl_2[8a] and *cis*-[Ru(6,6′-Cl_2bpy)$_2$(OH_2)$_2$](CF_3SO_3)$_2$[8b] have also been immobilised in MCM-41-type mesoporous silicas by the primary modification route (solvent impregnation). In the case of [Ru(bpy)$_3$]$^{2+}$, it was thought that the ions were adsorbed by a cation-exchange reaction with protons of silanol groups located on the mesopore surface. The interactions between the Ru^{II} ions and the surface were weak and it was found that when the samples were dehydrated, the adsorbed ions aggregated to cause self-quenching of luminescence. The luminescence was intensified upon hydration of the samples, indicating that the aggregated [Ru(bpy)$_3$]$^{2+}$ ions were dispersed in the mesopore to suppress self-quenching.

One way to control better the state and distribution of immobilised metal species on mesoporous silica is to graft the metal complexes onto a previously modified surface. Typically, functional alkyltrialkoxysilanes are used as precursors for the surface modification.[9] Amine functions grafted to the surface in this way have enabled the direct complexation of transition-metal species (Fe^{II}, Mn^{II}, Cu^{II}, Co^{II}, Zn^{II}),[10–12] and the immobilisation of ruthenium porphyrin[13] and perfluorophthalocyanine[14] complexes through apical coordinative ligation on the metal centres. However, it was reported that both [Ru(bpy)$_3$]$^{2+}$ and *cis*-[Ru(6,6′-Cl_2bpy)$_2$(OH_2)$_2$]$^{2+}$ cations cannot be immobilised in MCM-41 modified with amine functions.[8b]

Some of us recently described how donor nitrile functions grafted to the surface of MCM-41 permitted the immobilisation of dioxomolybdenum(VI) fragments.[15] In the present work we describe the use of the spacer ligand 4-(triethoxysilyl)butyronitrile for the derivatisation of MCM-41 with a Ru^{II} complex containing the thioether ligand 1,4,8,11-tetrathiacyclotetradecane ([14]aneS_4). The hybrid material has been fully characterised by means of elemental analysis, powder X-ray diffraction (XRD), N_2 adsorption, TGA, IR, UV/VIS and photoluminescence spectroscopy, and magic-angle spinning (MAS) NMR (^{13}C, ^{29}Si).

Experimental

General procedures and starting materials

All preparations and manipulations were performed using standard Schlenk techniques under an oxygen-free and water-free nitrogen atmosphere. Commercial grade solvents were dried and deoxygenated by refluxing over appropriate drying

 DOI: 10.1039/b101152i

agents under nitrogen atmosphere and distilled prior to use. Purely siliceous MCM-41 was synthesised as described previously using $[(C_{14}H_{29})NMe_3]Br$ as the templating agent.[2] After calcination (540 °C/6 h), the material was characterised by powder XRD, N_2 adsorption and FTIR spectroscopy. Prior to the grafting experiment, calcined MCM-41 was activated at 160 °C *in vacuo* (10^{-2} Pa) for 2 hours. This treatment is sufficient to achieve complete thermodesorption of physically adsorbed water molecules from the silica surface.[16] *cis*-$[Ru(DMSO)_4Cl_2]$ was prepared as described in the literature.[17]

Physical measurements

Microanalyses were obtained with a LECO CHNS-932 Elemental Analyser. IR spectra were obtained as KBr pellets using a FTIR Mattson-7000 infrared spectrophotometer. UV/VIS spectra were obtained at room temperature on a Jasco V-560 spectrophotometer. Solution spectra were measured in NCMe, DMSO or CH_2Cl_2 solutions. Diffuse reflectance UV/VIS spectra were obtained using a Jasco ISV-469 integrating sphere attachment. The photoluminescent data of the complexes, in the solid state, were performed in a Spex Fluorolog spectrofluorometer, model FL212 system, double grating 0.22 m Spex 1680 monochromators, and 450 W Xenon lamp as excitation source using the front face mode. This apparatus was fully controlled by a DM3000F spectroscopic computer. All conditions were kept constant (excitation and emission slits and wavelength excitation) for comparison purposes. Powder XRD data were collected on a Philips X'pert diffractometer using Cu-Kα radiation filtered by Ni. TGA studies were performed using a Mettler TA3000 system at a heating rate of 5 K min^{-1} under a static atmosphere of air. ^1H NMR spectra were recorded on a Bruker AMX spectrometer. Room temperature ^{29}Si and ^{13}C solid-state NMR spectra were recorded at 79.49 and 100.62 MHz respectively, on a (9.4 T) Bruker MSL 400P spectrometer. ^{29}Si MAS NMR spectra were recorded with 40° pulses, spinning rates 5.0–5.5 kHz and 60 s recycle delays. ^{29}Si CP MAS NMR spectra were recorded with 5.5 μs ^1H 90° pulses, 8 ms contact time, a spinning rate of 4.5 kHz and 4 s recycle delays. Chemical shifts are quoted in parts per million from TMS. ^{13}C CP MAS NMR spectra were recorded with a 4.5 μs ^1H 90° pulse, 2 ms contact time, a spinning rate of 8 kHz and 4 s recycle delays. Chemical shifts are quoted in parts per million from TMS.

Nitrogen adsorption isotherms were obtained at 77 K for pristine and derivatised MCM-41 materials. The experimental data were recorded gravimetrically using a CI electronic MK2-M5 microbalance. Equilibrium of each data point was monitored using CI electronics Labweigh software and the pressure was monitored using an Edwards Barocel pressure sensor. The pristine calcined MCM-41 was outgassed at 723 K whereas the derivatised sample was outgassed at a lower temperature of 413 K to minimise destruction of its functionalities. Both samples were held at the outgassing temperature overnight (>14 h), to give a residual pressure of *ca.* 10^{-4} mbar, and then cooled to room temperature prior to adsorption measurements. The BET specific surface area, S_{BET}, was evaluated from the data in the relative pressure range $P/P_0 = 0.05–0.25$. The cross-sectional area used in the BET calculations for a nitrogen molecule on the solid surface was 16.2 $Å^2$. The specific total pore volume (micropore plus mesopore, V_t) was evaluated from the nitrogen uptake at $P/P_0 \approx 0.95$, using the liquid nitrogen density of 0.8081 g cm^{-3}.

Preparation of ruthenium complexes

$[Ru([14]aneS_4)(DMSO)Cl]^+(Cl^-, PF_6^-)$ (1). The thioether macrocycle [14]aneS_4 (0.28 g, 1.03 mmol) was added to *cis*-$[Ru(DMSO)_4Cl_2]$ (0.50 g, 1.03 mmol) in dry ethanol (15 mL) and the suspension refluxed for 3 hours under a nitrogen atmosphere. The resulting pale yellow solution was concentrated to *ca.* 5 mL and addition of diethyl ether precipitated the product. The mother-liquor was filtered off and the remaining precipitate was washed with diethyl ether–hexane and dried *in vacuo* (0.44 g, 82%) (Found: C, 27.82; H, 5.00. $C_{12}H_{26}Cl_2ORuS_5$ requires C, 27.79; H, 5.05%); ν_{max}/cm^{-1} 2962m, 2917m and 2849w [ν(C–H)], 1427vs and 1402sh [δ(C–H)], 1080vs and 1019vs [ν(S=O), S coordinated], 427s [ν(Ru–S)], 377s [δ(C–S–O)] and 275m [ν(Ru–Cl)] (KBr); λ_{max}/nm (DMSO) 370 (ε/dm^3 mol^{-1} cm^{-1} 700) and 336 (540, sh); δ_H (300 MHz, CD_3CN, $SiMe_4$) 3.40–3.21 (m, [14]aneS_4), 3.31 (s, DMSO), 3.26 (s, DMSO), 3.07–2.91 (m, [14]aneS_4), 2.58–2.49 (m, [14]aneS_4) and 2.42–2.09 (m, [14]aneS_4).

Dissolution of this compound in the minimum amount of water and addition of 1 equivalent of NH_4PF_6 gave an abundant yellow precipitate $[Ru([14]aneS_4)(DMSO)Cl]PF_6$, which was filtered off, washed with water and diethyl ether, and dried *in vacuo*; ν_{max}/cm^{-1} 2982m, 2935m and 2847w [ν(C–H)], 1439vs, 1421vs and 1403sh [δ(C–H)], 1084vs [ν(S=O), S coordinated], 840vs and 558s (PF_6^-), 428s [ν(Ru–S)], 379s [δ(C–S–O)] and 273m [ν(Ru–Cl)] (KBr).

$[Ru([14]aneS_4)(NCMe)Cl]Cl$ (2). A solution of $[Ru([14]aneS_4)(DMSO)Cl]Cl$ (0.88 g, 1.70 mmol) in NCMe (50 mL) was refluxed for 30 min. After concentration to *ca.* 7 mL and addition of diethyl ether, the yellow crystalline complex that formed was filtered off and washed with diethyl ether (15 mL). Recrystallisation from NCMe–hexane–diethyl ether (4 : 1 : 3) gave, in one week, yellow crystals of **2** (0.79 g, 97%) (Found: C, 29.82; H, 4.71; N, 2.80. $C_{12}H_{23}Cl_2NRuS_4$ requires C, 29.93; H, 4.81; N, 2.91%); ν_{max}/cm^{-1} 2960m and 2911m [ν(C–H)], 2272w [ν(N≡C)], 1423vs and 1402s [δ(C–H)], 468s [ν(Ru–S)] and 278m [ν(Ru–Cl)] (KBr); λ_{max}/nm (NCMe) 367 (ε/dm^3 mol^{-1} cm^{-1} 500), 338 (490, sh) and 201 (36330); δ_H (300 MHz, CD_3CN, $SiMe_4$) 3.43–3.09 (m, [14]aneS_4), 3.02–2.73 (m, [14]aneS_4), 2.51–2.13 (m, [14]aneS_4) and 1.97 (3 H, s, NCMe).

$[Ru([14]aneS_4)(NC(CH_2)_3Si(OEt)_3)Cl]Cl$ (3). A solution of $[Ru([14]aneS_4)(DMSO)Cl]Cl$ (0.50 g, 0.96 mmol) in dry ethanol (30 mL) was treated with an excess of $NC(CH_2)_3Si(OEt)_3$ (2 mL) and refluxed for 60 min. After concentration to *ca.* 7 mL, addition of diethyl ether gave an oily complex that was filtered off and washed with diethyl ether (20 mL). Recrystallization from ethanol–CH_2Cl_2–diethyl ether (4 : 2 : 3) gave the product **3** as a yellow powder (0.57 g, 88%) (Found: C, 35.42; H, 6.01; N, 1.98; S, 19.32. $C_{20}H_{41}Cl_2NO_3RuS_4Si$ requires C, 35.76; H, 6.15; N, 2.08; S, 19.09%); ν_{max}/cm^{-1} 2970s and 2916s [ν(C–H)], 2248m [ν(N≡C)], 1429vs and 1406sh [δ(C–H)], 1081vs [ν(Si–O)], 463 and 427 [ν(Ru–S)] (KBr); λ_{max}/nm (CH_2Cl_2) 364 (ε/dm^3 mol^{-1} cm^{-1} 1210), 307 (1200) and 266 (3270, sh); δ_H (300 MHz, CD_2Cl_2, $SiMe_4$) 3.58 (q, OCH_2CH_3), 2.95–3.45 (m, [14]aneS_4), 2.71–2.76 (m, [14]aneS_4), 2.38–2.67 (m, [14]aneS_4 and $NCCH_2$), 1.65–1.80 (m, $CH_2CH_2CH_2$), 1.22 (t, OCH_2CH_3), 0.58 (CH_2Si). ^{29}Si MAS NMR spectrum exhibited one resonance at δ −53.5. ^{13}C CP MAS NMR: δ 129.1 (C≡*C*), 58.7 (–O*C*H_2–), 36.9, 30.9, 25.2 ([14]aneS_4), 18.7 (*C*H_3CH_2O–), 13.84, 11.3, 9.15 ($NC(CH_2)_3Si(OEt)_3$).

Immobilisation of ruthenium complex

$[Ru([14]aneS_4)(NC(CH_2)_3Si(OEt)_n)Cl]Cl$–MCM-41 (4). Calcined MCM-41 (0.5 g) was dehydrated and suspended in toluene (30 mL). It was then treated with a 0.05 M solution of $[Ru([14]aneS_4)(NC(CH_2)_3Si(OEt)_3)Cl]Cl$ in CH_2Cl_2 (15 mL). The mixture was stirred at room temperature for 1 day. The solution was filtered off and the yellow solid washed three times with 15 mL portions of CH_2Cl_2, before drying *in vacuo* (10^{-2} Pa) at room temperature for several hours (Found: C, 9.18; H, 2.47; N, 1.49; S, 7.03; Ru, 5.70%); ν_{max}/cm^{-1} 2985m and 2925m [ν(C–H)], 2254w [ν(N≡C)], 1435m, 1427sh and 1408m [δ(C–H)], 1087vs [ν(Si–O)], 463m and 427m [ν(Ru–S)] (KBr); λ_{max}/nm (diffuse reflectance) 370 and 303. ^{29}Si MAS NMR spectrum

exhibited one broad resonance at δ −108.7 (Q^4) and a shoulder at about δ −101 (Q^3). ^{29}Si CP MAS NMR: δ −107.9 (Q^4), −100.9 (Q^3), −91.8 (Q^2), −75 to −35 (br, T^m). ^{13}C CP MAS NMR: δ 59.0 (–O*C*H$_2$–), 36.5, 30.3, 24.6 ([14]aneS$_4$), 18.4 (*C*H$_3$CH$_2$O–), 13.1, 9.3 (NC(CH$_2$)$_3$Si(OEt)$_n$).

Results and discussion

Preparation and characterisation of Ru^{II} complexes

The reaction between *cis*-[Ru(DMSO)$_4$Cl$_2$] and the thioether ligand 1,4,8,11-tetrathiacyclotetradecane ([14]aneS$_4$) produced the complex [Ru([14]aneS$_4$)(DMSO)Cl]Cl (**1**), in a manner similar to that previously reported for [Ru([9]aneS$_3$)(DMSO)Cl$_2$][18] and [Ru([12]aneS$_4$)(DMSO)Cl]Cl (Scheme 1).[19] The FTIR spectrum of **1** exhibits bands for the S=O (1080 and 1019 cm^{-1}), Ru–S (427 cm^{-1}) and Ru–Cl (275 cm^{-1}) stretches that are similar to those seen in the related complex [Ru([12]aneS$_4$)(DMSO)Cl]Cl (1076 and 1020, 424 and 280 cm^{-1} respectively).[19] In the ^{1}H NMR spectrum, singlets were observed at δ 3.31 and 3.26 assigned to the protons of coordinated DMSO. The [14]aneS$_4$ ligand gives rise to a number of multiplets between δ 3.4 and 2.1.

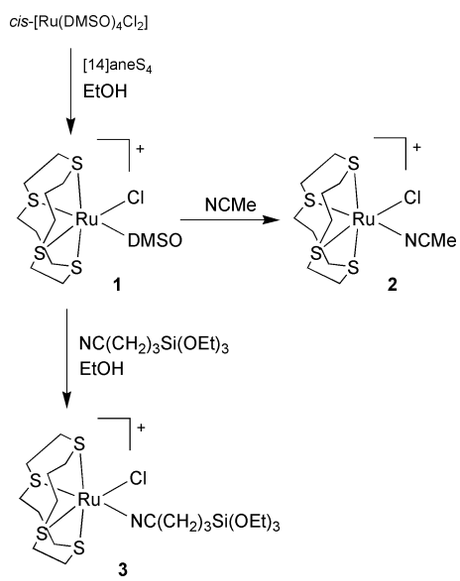

Scheme 1

The compound [Ru([14]aneS$_4$)(NCMe)Cl]Cl (**2**) was subsequently obtained by recrystallisation of [Ru([14]aneS$_4$)(DMSO)Cl]Cl (**1**) in acetonitrile–diethyl ether (Scheme 1). The FTIR spectrum of **2** exhibits bands for the C≡N (2272 cm^{-1}), Ru–S (468 cm^{-1}) and Ru–Cl (278 cm^{-1}) stretches. The singlet for the methyl protons of coordinated acetonitrile appears at δ 1.97 in the ^{1}H NMR spectrum. This synthesis method is generally applicable to the synthesis of a variety of complexes with monodentate and bidentate nitrogen donor ligands.[18–20] Thus, reaction of **1** with 4-(triethoxysilyl)butyronitrile in refluxing ethanol gave a yellow solution from which the product [Ru([14]aneS$_4$)(NC(CH$_2$)$_3$Si(OEt)$_3$)Cl]Cl (**3**) was isolated in good yield (Scheme 1). The FTIR spectrum of this complex displays the characteristic C≡N stretching band of the coordinated nitrile at 2248 cm^{-1}.

Synthesis and textural properties of MCM-41-supported Ru^{II}([14]aneS$_4$) complex

Treatment of MCM-41 with an excess of [Ru([14]aneS$_4$)(NC(CH$_2$)$_3$Si(OEt)$_3$)Cl]Cl (**3**) in a mixture of toluene–dichloromethane gave the Ru-modified mesoporous material **4** (Scheme 2). The product was isolated by filtration and washed thoroughly with dichloromethane to remove unreacted ruthenium complex before drying *in vacuo* at room temperature. Elemental analysis indicated that the pale yellow derivatised MCM contained approximately 5.7 mass% Ru (0.56 mmol g^{-1}). If the surface area is taken as 500 m^2 g^{-1} (see below), the metal content corresponds to a surface coverage of about 0.7 Ru atom per nm^2. This value is comparable to the concentration of surface silanol groups in pristine calcined MCM-41, reported to be in the range 1–3 per nm^2.[21,22] The Ru : C : S molar ratio found for **4** (1 : 14 : 4) indicates, firstly, that the {Ru[14]aneS$_4$Cl}$^+$ fragment remained intact during the immobilisation process and, secondly, that ethoxy groups were eliminated to form stable covalent bonds with the framework of MCM-41. TGA of material **4** showed that oxidative decomposition of the encapsulated ruthenium complex took place in air between 220 and 280 °C (13.4% mass loss), characterised by a very sharp, intense peak at 246 °C in the differential thermogravimetric (DTG) profile. The free complex **3** exhibited similar thermal behaviour, decomposing at 253 °C under the same conditions (59.9% mass loss between 220 and 280 °C).

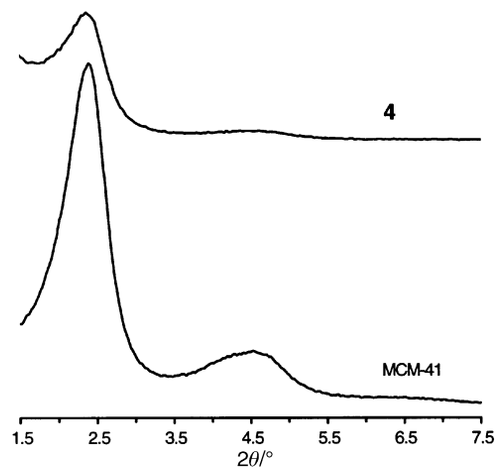

Fig. 1 Powder XRD patterns of pristine calcined MCM-41 and the functionalised sample [Ru([14]aneS$_4$)(NC(CH$_2$)$_3$Si(OEt)$_n$)Cl]Cl–MCM-41 **4**.

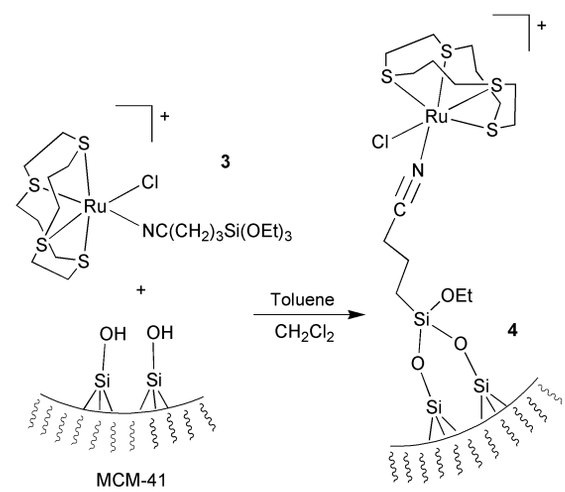

Scheme 2

Powder XRD. The XRD pattern of the pristine calcined MCM-41 contains the characteristic and intense low angle peak at d = 36.48 Å which can be indexed as the d_{100} reflection on a hexagonal unit cell ($a = 2d_{100}/3^{1/2}$ = 42.12 Å, Fig. 1). The pattern also displays a broad secondary feature at about 4.5° 2θ where (110) and (200) reflections would be expected for a hexagonally ordered material such as MCM-41. The absence of resolved peaks indicates that any structural order of the material did not extend over a long range. A very similar result was obtained by Schmidt *et al.* for a purely siliceous MCM-41

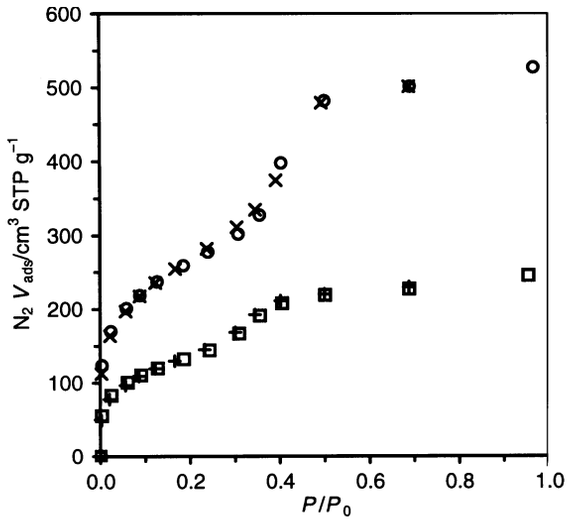

Fig. 2 N_2 adsorption–desorption isotherms at 77 K for pristine calcined MCM-41 [adsorption (○); desorption (×)] and the ruthenium-modified material **4** [adsorption (6); desorption (+)].

prepared as in this work using the surfactant $[(C_{14}H_{29})NMe_3]Br$.[23] Upon functionalisation with the ruthenium complex **3**, the position of the d_{100} reflection remained constant, suggesting no loss in the structural ordering of the hexagonal mesoporous host ($d = 36.40$ Å, $a = 42.02$ Å). There was however a significant reduction in the peak intensity. This is attributed to contrast matching between the amorphous silica framework and metal–organic moieties that are uniformly distributed inside the channels of MCM-41.[24]

Nitrogen adsorption studies at 77 K. The pristine siliceous MCM-41 sample gave a reversible type IV N_2 adsorption–desorption isotherm according to the IUPAC classification (Fig. 2), characteristic of mesoporous solids (intermediate pore size).[25] At low relative pressures ($P/P_0 \leq 0.3$) the adsorbed volume increases linearly with increasing pressure – this region corresponds to a monolayer–multilayer adsorption on the pore walls. Between $P/P_0 = 0.3$ and 0.4 there is a sharp increase in the adsorbed volume, characteristic of mesopore filling. The narrow range over which this occurs is consistent with a monodispersed size of the mesopores. At higher relative pressures multilayer adsorption takes place on the external surface, resulting in a gradual linear increase of the adsorbed volume. The BET specific surface area (S_{BET}) was calculated as 946 m^2 g^{-1} and the mesopore volume (V_p) as 0.81 cm^3 g^{-1}. These values are in agreement with published data.[26,27]

The N_2 adsorption isotherm of the modified MCM-41 was different from that of the unmodified material in that it displayed a considerably lower N_2 uptake. The value of S_{BET} decreased by 48% (to 495 m^2 g^{-1}) and that of V_P decreased by 53% (to 0.38 cm^3 g^{-1}). Nevertheless the isotherm was still of type IV. This indicates that the textural properties of the silica support were preserved during the grafting experiment and that the channels remained accessible. The lower P/P_0 coordinate of the inflection point and the less steep increase in the adsorbed volume in the N_2 adsorption isotherm has been previously associated with changes in pore size distribution due to immobilisation of bulky complexes on the internal silica surface of mesoporous hosts.[15,28] In summary, powder XRD and N_2 sorption studies are consistent with homogeneous lining of the pore walls by the anchored metal–organic species reducing the accessible diameter of the pores.

Spectroscopic studies of MCM-41-supported Ru^{II}([14]aneS$_4$) complex

IR and UV-VIS spectroscopy indicated that the structural integrity of the Ru^{II}([14]aneS$_4$) complex was retained after

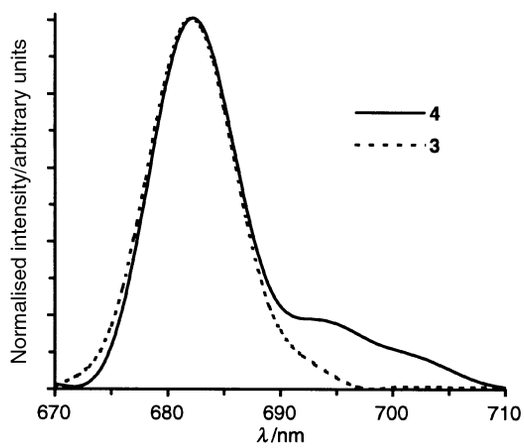

Fig. 3 Solid-state emission spectra at room temperature for [Ru([14]aneS$_4$)(NC(CH$_2$)$_3$Si(OEt)$_3$)Cl]Cl **3** and ruthenium-modified material **4**, $\lambda_{exc} = 370$ nm.

inclusion in MCM-41. IR bands at 463 and 427 cm^{-1} (ν_{Ru-S}) for the modified material **4** match those observed for the free complex **3**. In addition, the presence of the N-coordinated butyronitrile ligand in **4** is confirmed by the weak C≡N stretching band observed at 2254 cm^{-1}, which is shifted to slightly higher energy compared with that for **3** (2248 cm^{-1}). Complex **3** also absorbs at 2970 and 2916 cm^{-1}, corresponding to the ν_{C-H} vibrations of the [14]aneS$_4$ macrocycle and the triethoxysilylbutyronitrile tethering ligand. These two bands shift to 2985 and 2925 cm^{-1}, respectively, after reaction with MCM-41, which may indicate a more tense macrocycle ring or one with less freedom of vibration. In addition, the loss of ethoxide groups through reaction with surface silanols is expected to affect the IR spectrum in this region.

The UV/VIS spectrum of a solution of **3** in CH_2Cl_2 displays two bands at 364 and 307 nm. These were observed at almost the same energy in the diffuse reflectance spectrum. The modified MCM **4** displays a band at 370 nm, used for excitation of the sample in luminescence studies. The corresponding spectra are shown in Fig. 3 and it can be seen that both systems exhibit a main emission band at 682 nm, displaying a Gaussian shape. These results indicate that there is no significant structural change around the metal centre. The full-width-at-half-maximum (FWHM) of the band at 682 nm is 167.4 cm^{-1} and 151.7 cm^{-1} for **3** and **4** respectively. A preliminary test established that the lifetime of the emission was of the order of 10^{-6} s or less. This timescale is typical of metal-to-ligand-charge-transfer bands in systems comprising Ru^{II} complexes with unsaturated N-donor ligands.[29] The integrated area of the emission of **4** has an increase of 10% over **3** due to the gain in the 690–710 nm range, which reveals an improvement in the luminescent performance of the ruthenium complex when supported on MCM-41.

Solid-state MAS NMR studies. Fig. 4 shows the ^{29}Si MAS and CP MAS NMR spectra of pristine calcined MCM-41 and the modified material **4**. The support material, before functionalisation, displays two broad convoluted resonances in the CP MAS spectrum at δ −107.9 and −100.9, assigned to Q^4 and Q^3 species of the silica network respectively [$Q^n = Si(OSi)_n(OH)_{4-n}$]. A weak shoulder is also observed at δ −91.8 for the Q^2 species. Comparison of this spectrum with that of material **4** shows that the grafting process resulted in a reduction of the Q^3 and Q^2 resonances, and a concomitant increase of the Q^4 resonance. This is consistent with esterification of the free silanol groups (both single and geminal) by nucleophilic substitution at the silicon atom in the trialkoxysilylbutyronitrile spacer ligand. Fig. 4 shows that there are still a large number of unreacted Q^3 silicon atoms in **4**. These may be hydrogen-bonded silanols present at the surface, $(SiO)_3Si–OH–OH–Si(SiO)_3$, which have

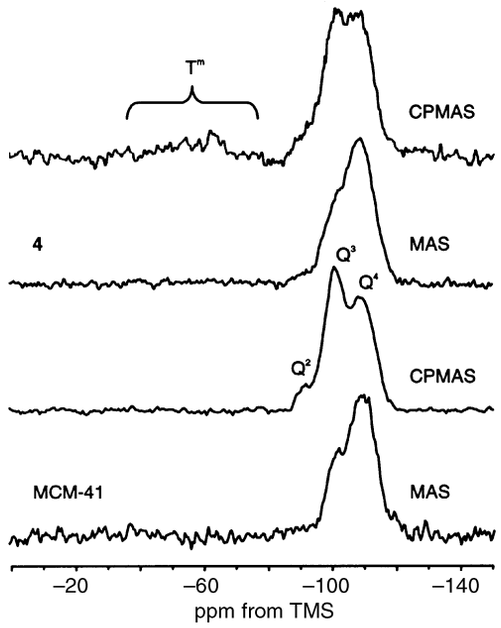

Fig. 4 ^{29}Si CP MAS and MAS NMR at room temperature of pristine calcined MCM-41 and the ruthenium-modified material **4**.

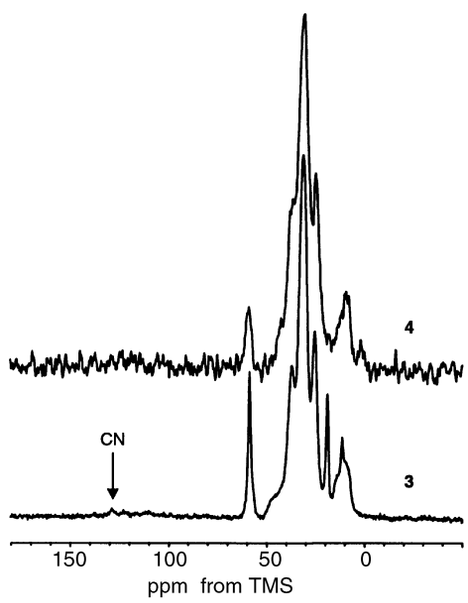

Fig. 5 ^{13}C CP MAS NMR at room temperature of [Ru([14]aneS$_4$)(NC(CH$_2$)$_3$Si(OEt)$_3$)Cl]Cl **3** and MCM-41 derivatised with **3** (**4**).

previously been shown to be unreactive to silyating agents.[21] A weak broad signal between δ −35 and −75, maximum intensity at about δ −63, is attributed to three resonances for the organosilica species [T^m = R*Si*(OSi)$_m$(OEt)$_{3-m}$, m = 1–3].[30] The liquid-state ^{29}Si NMR of neat NC(CH$_2$)$_3$Si(OEt)$_3$ exhibited one resonance at δ −45.6, while the solid-state ^{29}Si NMR of complex **3** gave one resonance at δ −53.5.

The solid-state ^{13}C CP MAS NMR spectra of [Ru([14]aneS$_4$)(NC(CH$_2$)$_3$Si(OEt)$_3$)Cl]Cl **3** and the Ru-modified MCM **4** are shown in Fig. 5. The resonances for the methylene carbons of the macrocycle and the cyanopropyl group (δ 25–37 and δ 9–14) do not change significantly as a result of the grafting reaction, confirming that the structural integrity of the complex was retained upon reaction with MCM-41. There is a slight broadening in the signals due to the range of chemically different environments in which the molecules are located, giving rise to an envelope of peaks with very similar chemical shifts. The main difference between the spectra of **3** and **4** is that, as expected, the resonances corresponding to CH$_3$– (δ 18.7) and –CH$_2$– (δ 58.7) of the ethoxide group are reduced in intensity as a result of the condensation reaction.[30] The presence of some residual ethoxide groups shows that the reaction was not complete and probably the major surface organosilica species in **4** corresponds to R*Si*(OSi)$_2$(OEt) (T^2). The ^{13}C CP MAS NMR spectrum of **3** exhibited one weak peak at δ 129 attributed to N*C*R. The corresponding resonance for **4** was not observed.

Conclusions

This work has demonstrated the versatile nature of the silane coupling agent 4-(triethoxysilyl)butyronitrile for creating functional monolayers on ordered mesoporous silica. The uniformly distributed pendant nitrile groups permit the immobilisation of bulky metal complexes, in this case a Ru^{II} thioether [14]aneS$_4$ complex, through a coordination bond to the metal centre. The textural properties of the support are preserved during the grafting experiment and the channels remain accessible. This method of immobilisation favours the formation of isolated active sites and should be applicable to a broad range of ruthenium(II) complexes including, for example, polypyridyl complexes. The luminescence characteristics of the complexes anchored in mesoporous silica are worth investigating to understand the nature of the mesopore as well as the states of the catalytically active sites on the mesopore. These studies are currently underway in our laboratories.

Acknowledgements

The authors are grateful to FCT, POCTI and FEDER for financial support (Project PCTI/1999/QUI/32889). J. M. and P. F. thank PRAXIS XXI for Ph.D. grants. I. S. G. acknowledges CRUP (Acções Integradas Programme) for generous support.

References

1 K. Moller and T. Bein, *Chem. Mater.*, 1998, **10**, 2950; T. Maschmeyer, *Curr. Opin. Solid State Mater. Sci.*, 1998, **3**, 71; R. A. Sheldon, I. W. C. E. Arends and H. E. B. Lempers, *Catal. Today*, 1998, **41**, 387.
2 C. T. Kresge, M. E. Leonowicz, W. J. Roth, J. C. Vartuli and J. S. Beck, *Nature*, 1992, **359**, 710; J. S. Beck, J. C. Vartuli, W. J. Roth, M. E. Leonowicz, C. T. Kresge, K. D. Schmitt, C. T.-W. Chu, D. H. Olson, E. W. Sheppard, S. B. McCullen, J. B. Higgins and J. L. Schlenker, *J. Am. Chem. Soc.*, 1992, **114**, 10834.
3 R. Burch, N. Cruise, D. Gleeson and S. C. Tsang, *Chem. Commun.*, 1996, 951.
4 T. Maschmeyer, F. Rey, G. Sankar and J. M. Thomas, *Nature*, 1995, **378**, 159.
5 P. Ferreira, I. S. Gonçalves, F. E. Kühn, M. Pillinger, J. Rocha, A. M. Santos and A. Thursfield, *Eur. J. Inorg. Chem.*, 2000, 551.
6 S. O'Brien, J. M. Keates, S. Barlow, M. J. Drewit, B. R. Payne and D. O'Hare, *Chem. Mater.*, 1998, **10**, 4088; P. Ferreira, I. S. Gonçalves, F. Mosselmans, M. Pillinger, J. Rocha and A. Thursfield, *Eur. J. Inorg. Chem.*, 2000, 97.
7 P. Ferreira, I. S. Gonçalves, F. E. Kühn, M. Pillinger, J. Rocha, A. Thursfield, W.-M. Xue and G. Zhang, *J. Mater. Chem.*, 2000, **10**, 1395.
8 (*a*) M. Ogawa, T. Nakamura, J. Mori and K. Kuroda, *J. Phys. Chem. B*, 2000, **104**, 8554; (*b*) A. K.-W. Cheng, W.-Y. Lin, S.-G. Li, C.-M. Che and W.-Q. Pang, *New J. Chem.*, 1999, **23**, 733.
9 D. Brunel, N. Bellocq, P. Sutra, A. Cauvel, M. Laspéras, P. Moreau, F. DiRenzo, A. Galarneau and F. Fajula, *Coord. Chem. Rev.*, 1998, **178–180**, 1085; D. Brunel, *Microporous Mesoporous Mater.*, 1999, **27**, 329.
10 J. Evans, A. B. Zaki, M. Y. El-Sheikh and S. A. El. Safty, *J. Phys. Chem. B*, 2000, **104**, 10271.
11 W. A. Carvalho, M. Wallau and U. Schuchardt, *J. Mol. Catal. A: Chem.*, 1999, **144**, 91.
12 J. F. Díaz, K. J. Balkus, Jr, F. Bedioui, V. Kurshev and L. Kevan, *Chem. Mater.*, 1997, **9**, 61.

13 C.-J. Liu, S.-G. Li, W.-Q. Pang and C.-M. Che, *Chem. Commun.*, 1997, 65; C. J. Liu, W.-Y. Yu, S.-G. Li and C.-M. Che, *J. Org. Chem.*, 1998, **63**, 7364.
14 S. Ernst and M. Selle, *Microporous Mesoporous Mater.*, 1999, **27**, 355.
15 P. Ferreira, I. S. Gonçalves, F. E. Kühn, A. D. Lopes, M. A. Martins, M. Pillinger, A. Pina, J. Rocha, C. C. Romão, A. M. Santos, T. M. Santos and A. A. Valente, *Eur. J. Inorg. Chem.*, 2000, 2263.
16 C. P. Jaroniec, R. K. Gilpin and M. Jaroniec, *J. Phys. Chem. B*, 1997, **101**, 6861; C. P. Jaroniec, M. Kruk, M. Jaroniec and A. Sayari, *J. Phys. Chem. B*, 1998, **102**, 5503.
17 I. P. Evans, A. Spencer and G. Wilkinson, *J. Chem. Soc., Dalton Trans.*, 1973, 204.
18 B. J. Goodfellow, V. Félix, S. M. D. Pacheco, J. Pedrosa de Jesus and M. G. B. Drew, *Polyhedron*, 1997, **16**, 393.
19 T. M. Santos, B. J. Goodfellow, J. Madureira, J. Pedrosa de Jesus, V. Félix and M. G. B. Drew, *New J. Chem.*, 1999, **23**, 1015.
20 B. J. Goodfellow, S. M. D. Pacheco, J. Pedrosa de Jesus, V. Félix and M. G. B. Drew, *Polyhedron*, 1997, **16**, 3293.
21 X. S. Zhao, G. Q. Lu, A. K. Whittaker, G. J. Miller and H. Y. Zhu, *J. Phys. Chem. B*, 1997, **101**, 6525.
22 P. L. Llewellyn, F. Schüth, Y. Grillet, F. Rouquerol, J. Rouquerol and K. K. Unger, *Langmuir*, 1995, **11**, 574.
23 R. Schmidt, M. Stöcker, E. Hansen, D. Akporiaye and O. H. Ellestad, *Microporous Mater.*, 1995, **3**, 443.
24 B. Marler, U. Oberhagemann, S. Voltmann and H. Gies, *Microporous Mater.*, 1996, **6**, 375.
25 S. J. Gregg and K. S. W. Sing, *Adsorption, Surface Area and Porosity*, Academic Press, London, 2nd edn., 1982.
26 M. D. Alba, A. Becerro and J. Klinowski, *J. Chem. Soc., Faraday Trans.*, 1996, **92**, 849.
27 A. A. Romero, M. D. Alba, W. Zhou and J. Klinowski, *J. Phys. Chem. B*, 1997, **101**, 5294.
28 D. Brunel, A. Cauvel, F. Fajula and F. DiRenzo, in *Zeolites: A Refined Tool for Designing Catalytic Sites*, ed. L. Bonneviot and S. Kaliaguine, Elsevier Science B. V., Amsterdam,1995, p. 173.
29 A. Juris, V. Balzani, F. Barigelletti, S. Campagna, P. Belser and A. von Zelewsky, *Coord. Chem. Rev.*, 1988, **84**, 85.
30 D. Derouet, S. Forgeard, J.-C. Brosse, J. Emery and J.-Y. Buzare, *J. Polym. Sci. A: Polym. Chem.*, 1998, **36**, 437.